



Jornal Brasileiro de Patologia e Medicina Laboratorial

ISSN: 1676-2444

ISSN: 1678-4774

Sociedade Brasileira de Patologia Clínica; Sociedade Brasileira de Patologia; Sociedade Brasileira de Citopatologia

Almeida, Vitor M.; Bezerra, Maximino Alencar; Nascimento, Jéssica C.; Amorim, Lidia Maria F.

Anticancer drug screening: standardization of *in vitro* wound healing assay

Jornal Brasileiro de Patologia e Medicina Laboratorial,  
vol. 55, no. 6, 2019, November-December, pp. 606-619

Sociedade Brasileira de Patologia Clínica; Sociedade Brasileira de Patologia; Sociedade Brasileira de Citopatologia

DOI: 10.5935/1676-2444.20190054

Available in: <http://www.redalyc.org/articulo.oa?id=393565199003>

- How to cite
- Complete issue
- More information about this article
- Journal's webpage in redalyc.org

UABM  
redalyc.org

Scientific Information System Redalyc

Network of Scientific Journals from Latin America and the Caribbean, Spain and Portugal

Project academic non-profit, developed under the open access initiative

# Anticancer drug screening: standardization of *in vitro* wound healing assay

## *Triagem de drogas anticâncer: padronização do ensaio de ranbura in vitro*

Vitor M. Almeida; Maximino Alencar Bezerra Jr.; Jéssica C. Nascimento; Lidia Maria F. Amorim

Universidade Federal Fluminense (UFF), Niterói, Rio de Janeiro, Brazil.

### ABSTRACT

**Introduction:** Gliomas are characterized by rapid proliferation and aggressive invasion into normal surrounding brain tissue. In medical laboratories, the *in vitro* wound healing assay stands out as a simple, easy, inexpensive and affordable method to evaluate cell migration and proliferation. **Objective:** To standardize the *in vitro* wound healing assay using antimicrotubule drugs as positive controls. **Methods:** U87MG glioma cells were seeded at different densities and, after 24 h, the monolayer was scratched using different micropipette tip size to create a gap with no cells. The cells were then treated with colchicine and paclitaxel in culture medium with the presence or absence of fetal bovine serum. The wound was photographed with the aid of an inverted microscope and the wound area was measured using the Image J software. **Results:** Better defined edges scratches and monolayer with approximately 90% confluence were obtained at  $1.5$  and  $2 \times 10^5$  cells/well density. The width and area of the scratch were, respectively,  $948 \mu\text{m}/2.193221 \text{ mm}^2$ ;  $964 \mu\text{m}/2.266 \text{ mm}^2$  and  $1448 \mu\text{m}/3.221 \text{ mm}^2$  to  $10$ ,  $200$  and  $1000 \mu\text{l}$  micropipette tips. Colchicine inhibited wound closure by  $12.6\%$  or  $3.4\%$ , both in the presence or absence of serum; paclitaxel  $2.4$  and  $6.7\%$  respectively. **Conclusion:** Under standardized conditions, colchicine and paclitaxel proved to be efficient positive controls into the *in vitro* wound healing assay.

**Key words:** colchicine; paclitaxel; glioma; cell proliferation; cell movement; antitumor drug screening assays.

### RESUMO

**Introdução:** Gliomas são caracterizados por terem rápida proliferação e invasão agressiva no tecido cerebral circundante normal. Em laboratórios médicos, o ensaio de ranbura – um teste *in vitro* – destaca-se por ser um método simples, fácil, barato e acessível para avaliar a migração e a proliferação celular. **Objetivo:** Padronizar o ensaio de ranbura, utilizando drogas antimicrotúbulos como controles positivos. **Métodos:** As células de glioma U87MG foram semeadas em diferentes concentrações e, após 24 horas, a monocamada foi arranhada usando ponteiros de diferentes tamanhos para criar uma fenda sem células. As células foram então tratadas com colchicina e paclitaxel, com meio em ausência ou presença de soro fetal bovino. A ranbura foi fotografada com auxílio de microscópio invertido, e a área da ranbura foi medida por meio do programa Image J. **Resultados:** Ranburas com bordas mais bem definidas e monocamada com aproximadamente 90% de confluência foram obtidas com  $1,5$  e  $2 \times 10^5$  células/poço. A largura e a área das ranburas obtidas foram, respectivamente,  $948 \mu\text{m}/2,193 \text{ mm}^2$ ;  $964 \mu\text{m}/2,266 \text{ mm}^2$ ; e  $1448 \mu\text{m}/3,221 \text{ mm}^2$  para as ponteiros de  $10$ ,  $200$  e  $1000 \mu\text{l}$ . A colchicina inibiu o fechamento das ranburas em  $12,6\%$  ou  $2,4\%$ , tanto na presença quanto na ausência de soro; o paclitaxel, em  $3,4\%$  e  $6,7\%$ , respectivamente. **Conclusão:** Em condições padronizadas, colchicina e paclitaxel podem ser usados como controles positivos eficientes no teste *in vitro* de ranbura.

**Unitermos:** colchicina; paclitaxel; glioma; proliferação celular; movimento celular; ensaios de seleção de medicamentos antitumorais.

## RESUMEN

**Introducción:** Gliomas se caracterizan por rápida proliferación e invasión agresiva del tejido cerebral normal circundante. En laboratorios médicos, el ensayo de cierre de herida – una prueba *in vitro* – se destaca por ser un método simple, fácil, de bajo costo y accesible para evaluar la migración y la proliferación celular. **Objetivo:** Estandarizar el ensayo de cierre de herida usando agentes anti-microtúbulos como control positivo. **Métodos:** Las células de glioma U87MG fueron sembradas en diferentes concentraciones y, después de 24 horas, la monocamada fue rayada con punteras de diferentes tamaños para crear una bendidura sin células. Las células fueron entonces tratadas con colchicina y paclitaxel, en medio con o sin suero fetal bovino. La ranura fue fotografiada con la ayuda de un microscopio invertido, y el área de la ranura fue medida mediante el programa Image J. **Resultados:** Ranuras con bordes más bien-definidos y monocamada con alrededor de 90% de confluencia se obtuvieron con  $1,5$  y  $2 \times 10^5$  células/pozo. La anchura y el área de las ranuras obtenidas fueron, respectivamente,  $948 \mu\text{m}/2,193 \text{ mm}^2$ ;  $964 \mu\text{m}/2,266 \text{ mm}^2$ ; y  $1448 \mu\text{m}/3,221 \text{ mm}^2$  para las punteras de  $10$ ,  $200$  y  $1000 \mu\text{l}$ . La colchicina inhibió el cierre de las ranuras en  $12,6\%$  o  $2,4\%$ , tanto en presencia como en ausencia de suero; el paclitaxel,  $3,4\%$  y  $6,7\%$ , respectivamente. **Conclusión:** En condiciones estandarizadas, colchicina y paclitaxel pueden ser usados como control positivo en el ensayo de cierre de herida *in vitro*.

**Palabras clave:** colchicina; paclitaxel; glioma; proliferación celular; movimiento celular; ensayos de selección de medicamentos antitumorales.

## INTRODUCTION

Methodologies for examining cell migration are very useful and important for a wide range of biomedical trials and exams, such as anti-cancer drug screening. Although there are several methods for visualizing cell migration in the field of laboratory medicine, such as Transwell/Boyden chamber assay, barrier assays, and microfluidics-based assays, these methods are often expensive and not accessible to all laboratories. The *in vitro* wound healing assay, also known as the “scratch assay” is a simple, versatile, and cost-effective method for studying cell migration. In this methodology, a cell-free area is generated in a confluent cell monolayer and the wound closure rate and cell migration can be quantified by time-lapsing photography with an inverted microscope at some time intervals<sup>(1)</sup>.

Cell migration is essential for many biological processes, such as tissue repair and regeneration; however, the aberrant regulation of this process drives the progression of many diseases, including cancer invasion and metastasis<sup>(2)</sup>. Cytoskeleton components, such as the actin and tubulin filaments, are crucial for cell migration. These proteins form highly versatile dynamic polymers, capable of organizing cytoplasmic organelles and intracellular compartments, defining cellular polarity and generating both protrusion and contraction forces<sup>(3,4)</sup>. Due to this, the cytoskeleton is considered one of the most promising targets in anticancer drug screening. Drugs capable of reaching both actin filaments<sup>(5)</sup>, such as the microtubule network, formed by tubulin<sup>(6)</sup>, are capable of promoting deregulation of cell structure and disruption of proliferative processes.

It is predicted that there will be 23.6 million new cancer cases worldwide each year by 2030, if recent trends in major cancers incidence and population growth are seen globally in the future. This is 68% more cases than in 2012, with slightly higher growth in low and medium human development index (HDI) countries (66% more cases in 2030 than in 2012) than in high and very high HDI countries (56% more cases in 2030 than in 2012)<sup>(7)</sup>. Glioblastoma is a malignant astrocytic glioma associated with poor prognoses because of their ability to migrate and diffusely infiltrate into the brain parenchyma. After the surgical resection of this type of tumor, the residual population of invasive cells gives rise to a recurrent tumor which, in more than 90% of cases, develops immediately adjacent to the resection margin or within several centimeters of the resection cavity<sup>(8)</sup>.

The purpose of this work was to standardize the wound healing assay to be used in the evaluation of substances with proliferative and migratory activity on glioma and other cancer cells. Colchicine<sup>(9-11)</sup> and paclitaxel<sup>(12-15)</sup>, which present antimicrotubules activity, were used as positive controls since they are capable of destabilizing and stabilizing microtubules, respectively.

## METHODS

### Cell culture

The human glioblastoma (GBM) cell line U87MG (ATCC®HTB-14™) was preserved in DMEM/F12 medium supplemented

with 10% of heat-inactivated fetal bovine serum, 100 units/ml penicillin, and 100 µg/ml streptomycin. The cells were preserved in humid atmosphere with 5% CO<sub>2</sub> at 37°C.

### Plate seeding and monolayer scratch

The U87MG cell line was trypsinized, counted at different cell concentrations (0.5; 1; 1.5; 2; 2.5 and  $3 \times 10^5$  cells/500 µl) and seeded on 24-well plate. After 24 hours of incubation at 37°C the monolayers were scratched, creating a cell-free gap, using a sterile micropipette tip at an angle of about 90 degrees to keep the scratch width limited. To determine the appropriate scratch size, three different micropipette tips sizes (1000, 200 and 10 µl) were used. Medium was removed and the wells were washed twice with serum free medium (500 µl) to remove floating cells by aspiration.

### Wound healing assay

Paclitaxel 10 µM (Sigma)<sup>(15)</sup> and colchicine 1 µM (Sigma)<sup>(16)</sup> were diluted in DMEN/F12 medium and used as positive assay controls in the presence (10%) or absence of bovine fetal serum, using  $1.5 \times 10^5$  cells/500 µl/well to form the cell monolayer. Cells treated with medium (500 µl), supplemented with or with no serum were used as negative control.

### Wound area quantification

The wound area was photographed using an inverted microscope (Bel Photonics inv 100) prior to addition of the drug (time 0), as well as after 24 h of the treatment, using an objective lens that allows viewing both scratch edges with 40× magnification. The images were saved as \*.tif files. To obtain the same field during the image acquisition, the reference points were made by drawing a straight line with an ultrafine tip pen marker, on the outer bottom of the plate wells. The reference mark was placed outside the capture image field but within the microscope field of view. Two scratch areas; above and below the guideline, were measured on each well at 0 and 24 h of treatment using the Image J (software 1.48q, Rayne Rasband, National Institutes of Health, USA; <http://rsb.info.nih.gov/ij/>)<sup>(17)</sup>. Image J software was used to automatically detect the edge end position<sup>(18)</sup> and the entire procedure was described in the Supplementary Material. Wound closure (%) was quantified using the percentage change in the normalized measurement area divided by the original open area according to: Wound Closure % =  $[A(0) - A(t)/A(0)] \times 100$ <sup>(18)</sup> where the area at time zero (0) and the area after incubation time (t) were used to calculate the wound closure percentage.

### Statistical analysis

The results were expressed as a percentage of wound closure, considering the area measured at zero time as 0%. Comparisons between treatments were performed using analysis of variance test (ANOVA) followed by multiple comparison of Dunnett's test (three data sets were evaluated) using no treated cells as control. Data are presented as mean ± standard deviation (SD) and the  $p < 0.05$  was considered significant. Graphs and statistical analyses were performed using GraphPad Prism Software, version 5.0 (San Diego, CA, USA).

## RESULTS

### Wound

The steps performed for the *in vitro* wound healing assay were described in **Figure 1**. The ideal density for the U87MG cell line was 1.5 and  $2 \times 10^5$  cells (**Figure 2A**). Below this cell density, the confluence was lower than 90%, and above this, cells began to overlap and detach from the plate during the experiment. Different cell concentrations were also scratched with three micropipette tip sizes. The goal was to create a straight-edged, cell-free zone through the cell monolayer to be visualized and photographed after 24 hours. Cell density has a great influence on a homogeneous scratch. As cell concentration increased, the edges of the scratch

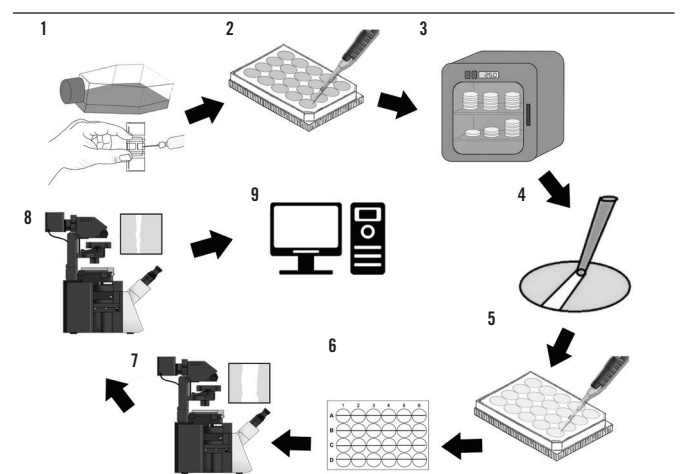


**FIGURE 1** — Steps to perform the *in vitro* wound healing assay

1. cell culture trypsinization and counting; 2. multi well plate seeding; 3. cells were allowed to attach, spread, and form a 90% confluent monolayer within a 24 hour period; 4. scratch-making; 5. wells washed with ice-cold PBS and drug application in medium with or without FBS; 6. draw a straight line on the bottom of the plates; 7. image capturing and gap measurement time = 0 h; 8. incubation and image capturing and gap measurement time = 24 h; 9. data analysis.

PBS: Phosphate buffered saline; FBS: fetal bovine serum.

began to form cell clusters that could disrupt the quantification of the scratch and also, at lower cell concentration, notches were created on the edge of scratch surface (**Figure 2B**). At  $1.5$  and  $2 \times 10^5$  cells the three micropipette tips were efficient to perform the wound (**Figure 2B**) differing only in the area ( $p < 0.05$ ). Scratch areas were  $1.908$ ,  $2.508$  and  $2.787 \text{ mm}^2$  to white ( $10 \mu\text{l}$ ), yellow ( $200 \mu\text{l}$ ) and blue ( $1000 \mu\text{l}$ ) micropipette tips, respectively. Even in the presence of serum (**Figure 3A e 3B**) the gaps performed

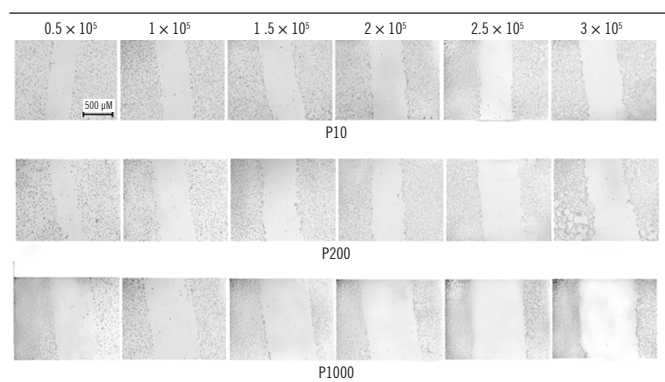


**FIGURE 2** – U87MG cell monolayer and *in vitro* wound healing assay standardization

A) U87MG cells were plated at different densities and after 24 hours of incubation, they were photographed to observe the confluence of cell monolayers. At  $0.5$  and  $1 \times 10^5$  cells per well the cellular monolayer presented low confluence and at  $2.5$  and  $3 \times 10^5$  cells per well the cells began to overlap each other; B) the monolayer was then wound wounded with three micropipette tips sizes. The  $1.5$  and  $2 \times 10^5/500 \mu\text{l}$  cell densities presented optimal confluence to perform the assay.

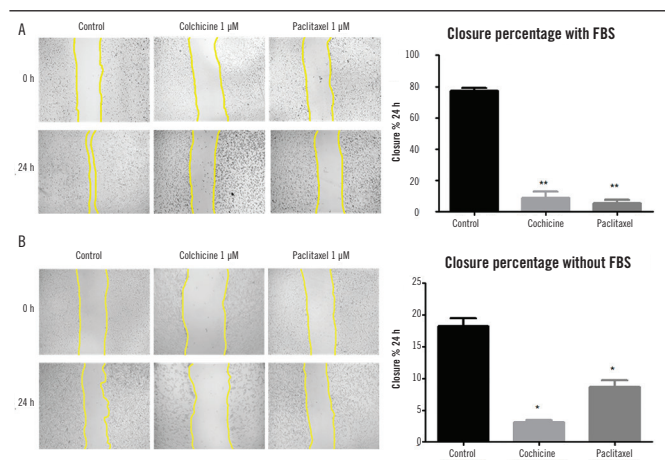


**FIGURE 3** – *In vitro* closure of the wound healing assay area after 24 hours colchicine or paclitaxel treatment in the presence or absence of serum

U87MG cells were plated at  $1.5 \times 10^5$  cells/well and treated for 24 hours with  $1 \mu\text{M}$  colchicine or  $1 \mu\text{M}$  paclitaxel diluted in DMEN/F12 with (A) or with no (B) serum. Images were captured by a camera coupled to the Bel view inv 100 microscope, with  $40\times$  magnification, before treatment (time-0) and after 24 hours of the treatment, and compared with the negative control with no drugs. The images were analyzed using the Image J software to evaluate the scratch by quantification of the areas occupied by the lesion. The graph shows the average values and the standard error of three experiments in quadruplicates. Test Anova followed by Dunnett post-boc test; \*\*\* $p < 0.001$ .

Anova: analysis of variance; FBS: fetal bovine serum.

using white micropipette tip were not completely closed after 24 hours of incubation; we chose to perform the experiments using the white tip because it had the smallest scratched area between the two other tips tested on the wells.

## Colchicine and tubulin as controls of wound assay

The wound healing assay was performed using colchicine and paclitaxel drugs diluted in medium with (Figure 3A) or with no (Figure 3B) fetal bovine serum (10%). Both drugs were capable to inhibit cell migration in the presence or absence of serum ( $p < 0.05$ ) and the presence of serum had no influence on the scratch area ( $p > 0.05$ ).

## DISCUSSION

### U87MG cell monolayer and scratching standardization

Although the *in vitro* wound assay is straight gap, the lack of standardization in its execution makes it difficult to compare results and reproduce experiments. The number of cells required to form a 90% confluent monolayer<sup>(19-21)</sup> needs to be determined according to the cell type and the size of plate wells. The cell lineage chosen for the study was U87MG, an established human glioblastoma strain, characterized by its high proliferation and migration rate<sup>(22, 23)</sup>, with population doubling time of approximately 34 h (ATCC, 2012) and size of  $12\text{--}14 \mu\text{m}$  (<http://bionumbers.hms.harvard.edu>). In the literature, the wound healing assay were described with different cell types, such as fibroblast cells<sup>(24, 25)</sup> and cancer cells, including glioblastoma<sup>(26-28)</sup>, breast cancer<sup>(20, 21, 29)</sup>, ovarian cancer<sup>(30-32)</sup>. Moreover, a large variation in the number of cells used for obtaining the cell monolayer to be scratched as  $1 \times 10^5$ <sup>(21, 30)</sup>,  $2 \times 10^5$ <sup>(29, 33)</sup> and  $1 \times 10^6$ <sup>(19, 34)</sup>, was found. Other authors described that cells were plated to obtain a confluence of 90% in the multiwell plates<sup>(19-21)</sup>. The use of U87MG cells in the wound healing assay has also been found in the literature<sup>(35)</sup>, however using 6-wells plates. Wound healing assay can be performed on any plate configuration available. Using 24-well plates achieves rapid screening compared to 12 or 6-well plates; these approaches minimize testing costs by reducing the amounts of test compound and reagent used. The ideal U87MG cell line density range was  $1.5$  and  $2 \times 10^5$ , corresponding to  $80\text{--}107 \times 10^3 \text{ cells/cm}^2$  and, although this density could be used as a reference, the assay should be adjusted according to the particular cell type to be studied.

To simulate tissue wound, the most common approach is to create a gap by scratching a confluent monolayer with a pipette



tip, needle, or other sharp tool. The size of micropipette tips used to produce the scratch also varied<sup>(26, 35-37)</sup>. All three tip sizes were efficient to promote the wound as previously reported<sup>(26, 35-37)</sup>. However, as the cell concentration increased, the less homogeneous the scratch became, forming cell clusters at the edges of the scratch. As the scratch is created manually, reproducible scratches may be difficult to produce. It is important to angle the pipette correctly, as well as to apply consistent pressure to create a consistent gap width. It is also important to wash twice with phosphate-buffered saline or free serum medium before treatment and image acquisition begin. Washing will remove debris from damaged or dead cells, particularly after mechanical scratching.

To reduce the risk of cell proliferation and compromise the study of migration, a low dose of mitomycin C proliferation inhibitor may be used. Mitomycin C (2-10 µg/ml) to stop proliferation for 2-5 h before scratching, an antitumor antibiotic that causes deoxyribonucleic acid (DNA) cross-linking and DNA synthesis inhibition, can be used to stop mitosis at various stages. However, the dose needs to be carefully optimized to avoid toxic effects that may affect cell migration. The most common method for suppressing cell proliferation in wound healing assays is the use of low serum concentrations or complete absence of fetal bovine serum in cell medium (serum deprivation). However, the duration of serum deprivation and the required serum concentrations need to be rigorously determined for each cell line studied, since primary cells do not tolerate serum deprivation as well as established cell lines.

The drugs chosen to be tested were colchicine and paclitaxel. Both are known drugs with activity on the microtubules<sup>(38, 39)</sup> and have proven action on migration<sup>(39, 40)</sup> and cell proliferation<sup>(41, 42)</sup>. In the literature there is a wide variation in both concentration and exposure time of these drugs tested in different cell types. In the standardization of the wound healing assay, the concentrations of 1 µM for colchicine<sup>(43)</sup> and 1 µM for paclitaxel<sup>(44)</sup> were established based on the literature. Both colchicine and paclitaxel demonstrated to be a good choice of positive controls for the achievement of the wound healing assay even in the presence of 10% serum.

## REFERENCES

1. Liang CC, Park AY, Guan JL. In vitro scratch assay: a convenient and inexpensive method for analysis of cell migration in vitro. *Nat Protoc.* 2007; 2(2): 329-33. PubMed PMID: 17406593.
2. Condeelis J, Singer RH, Segall JE. The great escape: when cancer cells hijack the genes for chemotaxis and motility. *Annu Rev Cell Dev Biol.* 2005; 21(1): 695-718. PubMed PMID: 16212512.

## Scratch gap area quantification

Cell migration can be quantified using the average distance of scratch width between its edges. Many measurements are required due to the irregularity of the edges and this manual quantification can be very time consuming. Scratch width (mm) should decrease as cell migration progresses over time. Cell migration can also be measured using the scratch areas. The scratch area can be calculated by manually or automatically tracing the cell-free area in images captured using the Image J software, public domain (NIH, Bethesda, MD). Different types of mathematical formulas were used to assess the gap closure at different periods of time. Some use formulas which results are presented using metric scales. The length measurement units can generate ambiguity when converting the proportions of a digital image (represented by pixels) to mm. Therefore, the representation of a result that does not use of length-based units, as the one used in this study, can help overcome the problem. Under normal conditions, the scratch area (mm or pixel) will decrease over time [scratch area =  $A(0) - A(t)/t$ ]. Alternatively, migration may be expressed as the percentage change in normalized measurement area to the original open area [wound closure % =  $A(0) - A(t)/A(0) \times 100$ ].

Quantifying the manual scratch using imaging software provides greater accuracy in the gap area values, taking into account the different edges irregularities provided by the implementation of manual or automatic measurement. Other software, other than the Image J, are used in the literature, and have also been efficient in these issues because they have quantification tools similar to Image J<sup>(18)</sup>.

## CONCLUSION

Standardization of the wound healing assay using a 24-multiwell plate glioma cell line was successful. Both colchicine and paclitaxel showed inhibition of monolayer gap closure even in the presence of 10% serum and can be used as positive controls of the technique. Therefore, standardized glioma technique can be accessible in many clinical and medical laboratories, with little or no use limitations.

3. Fife CM, McCarroll JA, Kavallaris M. Movers and shakers: cell cytoskeleton in cancer metastasis. *Br J Pharmacol.* 2014; 171(24): 5507-23. PubMed PMID: 24665826.
4. Hall A. The cytoskeleton and cancer. *Cancer Metastasis Rev.* 2009; 28(1-2): 5-14. PubMed PMID: 19153674.
5. Stehn JR, Haass NK, Bonello T, et al. A novel class of anticancer compounds targets the actin cytoskeleton in tumor cells. *Cancer Res.* 2013; 73(16): 5169-82. PubMed PMID: 23946473.

6. Zhou J, Giannakakou P. Targeting microtubules for cancer chemotherapy. *Curr Med Chem Anticancer Agents*. 2005; 5: 65-71. PubMed PMID: 15720262.
7. Manuscript A. Europe PMC Funders Group The Global Burden of Cancer 2013. *JAMA Oncol*. 2015; 1(4): 505-27. PubMed PMID: 26181261.
8. Lefranc F, Brotchi J, Kiss R. Possible future issues in the treatment of glioblastomas: special emphasis on cell migration and the resistance of migrating glioblastoma cells to apoptosis. *J Clin Oncol*. 2005; 23(10): 2411-22. PubMed PMID: 15800333.
9. Malawista SE, Bensch KG. Human polymorphonuclear leukocytes: demonstration of microtubules and effect of colchicine. *Science*. 1967; 156(3774): 521-2. PubMed PMID: 6021678.
10. Bhattacharyya B, Panda D, Gupta S, Banerjee M. Antimitotic activity of colchicine and the structural basis for its interaction with tubulin. *Med Res Rev*. 2008; 28(1): 155-83. PubMed PMID: 17464966.
11. Sivakumar G. Colchicine semisynthetics: chemotherapeutics for cancer? *Curr Med Chem*. 2013; 20(7): 892-8. PubMed PMID: 23210778.
12. Bensch KG, Malawista SE. Microtubule crystals: A new biophysical phenomenon induced by vinca alkaloids. *Nature*. 1968; 218(5147): 1176-7. PubMed PMID: 5656643.
13. de Brabander M, Geuens G, Nuydens R, Willebrords R, de Mey J. Taxol induces the assembly of free microtubules in living cells and blocks the organizing capacity of the centrosomes and kinetochores. *Proc Natl Acad Sci*. 1981; 78(9): 5608-12. PubMed PMID: 6117858.
14. Weaver BA. How taxol/paclitaxel kills cancer cells. *Mol Biol Cell*. 2014; 25(18): 2677-81. PubMed PMID: 25213191.
15. Liebmann JE, Cook JA, Lipschultz C, Teague D, Fisher J, Mitchell JB. Cytotoxic studies of paclitaxel (Taxol) in human tumour cell lines. *Br J Cancer*. 1993; 68(6): 1104-9. PubMed PMID: 7903152.
16. Cronstein BN, Molad Y, Reibman J, Balakhane E, Levin RI, Weissmann G. Colchicine alters the quantitative and qualitative display of selectins on endothelial cells and neutrophils. *J Clin Invest*. 1995; 96(2): 994-1002. PubMed PMID: 7543498.
17. Menon MB, Ronkina N, Schwermann J, Kotlyarov A, Gaestel M. Fluorescence-based quantitative scratch wound healing assay demonstrating the role of MAPKAPK-2/3 in fibroblast migration. *Cell Motil Cytoskeleton*. 2009; 66(12): 1041-7. PubMed PMID: 19743408.
18. Treloar KK, Simpson MJ. Sensitivity of edge detection methods for quantifying cell migration assays. *PLoS One*. 2013; 8(6). PubMed PMID: 23826283.
19. Dasari VR, Kaur K, Velpula KK, et al. Up regulation of PTEN in glioma cells by cord blood mesenchymal stem cells inhibits migration via downregulation of the PI3K/Akt pathway. *PLoS One*. 2010; 5(4). PubMed PMID: 20436671.
20. Oxmann D, Held-Feindt J, Stark AM, Hattermann K, Yoneda T, Mentlein R. Endoglin expression in metastatic breast cancer cells enhances their invasive phenotype. *Oncogene*. 2008; 27(25): 3567-75. PubMed PMID: 18223685.
21. Yang N, Hui L, Wang YAN, Yang H, Jiang X. SOX2 promotes the migration and invasion of laryngeal cancer cells by induction of MMP-2 via the PI3K/Akt/mTOR pathway. 2014; 2651-9. PubMed PMID: 24700142.
22. Jan H, Lee C, Shih Y, et al. Osteopontin regulates human glioma cell invasiveness and tumor growth in mice. 2010; 12(1): 58-70. PubMed PMID: 20150368.
23. Papi A, Bartolini G, Ammar K, et al. Inhibitory effects of retinoic acid and IIF on growth, migration and invasiveness in the U87MG human glioblastoma cell line. *Oncol Rep*. 2007; 18(4): 1015-21. PubMed PMID: 17786368.
24. Choritz L, Grub J, Wegner M, Pfeiffer N, Thieme H. Paclitaxel inhibits growth, migration and collagen production of human Tenon's fibroblasts – potential use in drug-eluting glaucoma drainage devices. 2010; 197-206. PubMed PMID: 19898860.
25. Ramírez G, Hagood JS, Sanders Y, et al. Absence of Thy-1 results in TGF- $\beta$  induced MMP-9 expression and confers a profibrotic phenotype to human lung fibroblasts. *Lab Invest*. 2011; 91(8): 1206-18. PubMed PMID: 21577212.
26. Cheng WY, Chiao MT, Liang YJ, Yang YC, Shen CC, Yang CY. Luteolin inhibits migration of human glioblastoma U-87 MG and T98G cells through downregulation of Cdc42 expression and PI3K/AKT activity. *Mol Bio Rep*. 2013; 40(9): 5315-26. PubMed PMID: 23677714.
27. Lu Y, Jiang F, Zheng X, et al. TGF- $\beta$ 1 promotes motility and invasiveness of glioma cells through activation of ADAM17. *Oncol Rep*. 2011; 25(5): 1329-35. PubMed PMID: 21359495.
28. Wesolowska A, Kwiatkowska A, Slomnicki L, et al. Microglia-derived TGF-beta as an important regulator of glioblastoma invasion – an inhibition of TGF-beta-dependent effects by shRNA against human TGF-beta type II receptor. *Oncogene*. 2008; 27(7): 918-30. PubMed PMID: 17684491.
29. Fortunati N, Marano F, Bandino A, Frairia R, Catalano MG, Boccuzzi G. The pan-histone deacetylase inhibitor LBH589 (panobinostat) alters the invasive breast cancer cell phenotype. *Int J Oncol*. 2014; 589(20): 700-8. PubMed PMID: 24366407.
30. de Jong E, Winkel P, Poelstra K, Prakash J. Anticancer effects of 15d-prostaglandin-J 2 in wild-type and doxorubicin-resistant ovarian cancer cells: novel actions on SIRT1 and HDAC. *PLoS One*. 2011; 6(9). PubMed PMID: 21957481.
31. Du F, Wu X, Liu Y, et al. Acquisition of paclitaxel resistance via PI3K – dependent epithelial – mesenchymal transition in A2780 human ovarian cancer cells. *Oncol Rep*. 2013; 1113-8. PubMed PMID: 23807572.
32. Kim BR, Yoon K, Byun HJ, Seo SH, Lee SH, Rho SB. The anti-tumor activator sMEK1 and paclitaxel additively decrease expression of HIF-1 $\alpha$  and VEGF via mTORC1-S6K/4E-BP-dependent signaling pathways. *Oncotarget*. 2014; 5(15): 6540-51. PubMed PMID: 25153728.
33. Moreno-Bueno G, Peinado H, Molina P, et al. The morphological and molecular features of the epithelial-to-mesenchymal transition. *Nat Protoc*. 2009; 4(11): 1591-613. PubMed PMID: 19834475.
34. Zhou Y, Su J, Shi L, Liao Q, Su QI. DADS downregulates the Rac1-ROCK1/PAK1-LIMK1-ADF/cofilin signaling pathway, inhibiting cell migration and invasion. *Oncol Rep*. 2013; 605-12. PubMed PMID: 23233092.
35. Gu JJ, Gao GZ, Zhang SM. MiR-218 inhibits the migration and invasion of glioma u87 cells through the slit-robo1 pathway. *Oncol Lett*. 2015; 9(4): 1561-6. PubMed PMID: 25789001.
36. Yu K, Chen Z, Pan X, et al. Tetramethylpyrazine-mediated suppression of C6 gliomas involves inhibition of chemokine receptor CXCR4 expression. *Oncol Rep*. 2012; 955-60. PubMed PMID: 22710373.

37. Guo P, Lan J, Ge J, Mao Q, Qiu Y. ID1 regulates U87 human cell proliferation and invasion. *Oncol Lett.* 2013; 6(4): 921-6. PubMed PMID: 24137437.
38. Yang H, Ganguly A, Cabral F. Inhibition of cell migration and cell division correlates with distinct effects of microtubule inhibiting drugs. *J Biol Chem.* 2010; 285(42): 32242-50. PubMed PMID: 20696757.
39. Goldman RD. The role of three cytoplasmic fibers in bhk-21 cell motility. I. Microtubules and the effects of colchicine. *J Cel Biol.* 1971; 51: 752-62. PubMed PMID: 4942774.
40. Salum LB, Altei WF, Chiaradia LD, et al. Cytotoxic 3,4,5-trimethoxychalcones as mitotic arresters and cell migration inhibitors. *Eur J Med Chem.* Elsevier Masson SAS; 2013; 63: 501-10. PubMed PMID: 23524161.
41. Salai M, Segal E, Cohen I, et al. The inhibitory effects of colchicine on cell proliferation and mineralisation in culture. *J Bone Joint Surg Br.* 2001; 83(6): 912-5. PubMed PMID: 11521938.
42. Jia L, Zhang S, Ye Y, et al. Paclitaxel inhibits ovarian tumor growth by inducing epithelial cancer cells to benign fibroblast-like cells q, qq. *Cancer Lett.* Elsevier Ireland Ltd; 2012; 326(2): 176-82. PubMed PMID: 22902993.
43. Lemor M, de Bustros S, Glaser BM. Low-dose colchicine inhibits astrocyte, fibroblast, and retinal pigment epithelial cell migration and proliferation. *Arch Ophthalmol.* 1986; 104(8): 1223-5. PubMed PMID: 3741255.
44. Westerlund A, Hujanen E, Höyhty M, Puistola U, Turpeenniemi-hujanen T. Ovarian cancer cell invasion is inhibited by paclitaxel. *Clin Exp Metastasis.* 1997; 15(3): 318-28. PubMed PMID: 9174131.

---

#### CORRESPONDING AUTHOR

Vitor Martins de Almeida  0000-0001-7902-6876  
e-mail: vitoralmeida1808@gmail.com



This is an open-access article distributed under the terms of the Creative Commons Attribution License.